LETTERS
PUBLISHED ONLINE: 23 MARCH 2015 | DOI: 10.1038/NCLIMATE2567
nature climate change

Positive but variable sensitivity of August surface ozone to large-scale warming in the southeast United States

Tzung-May Fu[1]*, Yiqi Zheng[1,2], Fabien Paulot[3,4], Jingqiu Mao[3,4] and Robert M. Yantosca[5]

Surface ozone, a major air pollutant toxic to humans and damaging to ecosystems[1,2], is produced by the oxidation of volatile organic compounds in the presence of nitrogen oxides ($NO_x = NO + NO_2$) and sunlight. Climate warming may affect future surface ozone levels[3–6] even in the absence of anthropogenic emission changes, but the direction of ozone change due to climate warming remains uncertain over the southeast US and other polluted forested areas[3–10]. Here we use observations and simulations to diagnose the sensitivity of August surface ozone to large-scale temperature variations in the southeast US during 1988–2011. We show that the enhanced biogenic emissions and the accelerated photochemical reaction rates associated with warmer temperatures both act to increase surface ozone. However, the sensitivity of surface ozone to large-scale warming is highly variable on interannual and interdecadal timescales owing to variation in regional ozone advection. Our results have important implications for the prediction and management of future ozone air quality.

Summertime surface ozone production over polluted forested areas is often dominated by the photochemical oxidation of biogenic isoprene (C_5H_8), whose emission from vegetation is nonlinearly dependent on temperature and sunlight intensity[11], and thus highly sensitive to climate warming. Previous climate–chemistry model (CCM) studies predicted surface ozone changes due to climate warming ($\Delta_{CW}O_3$) by simulating two climate scenarios—one for a future time slice and one for the present-day—in the absence of anthropogenic emission changes. These predictions showed no consensus on even the sign of $\Delta_{CW}O_3$ over polluted forested areas, such as the southeast US (SEUS), western Europe, and parts of East and South Asia[3–9]. This lack of consensus has been attributed to the uncertain model assumptions regarding ozone precursor (particularly isoprene) chemistry[4,5,7,12], as well as the different predictions of regional climate changes (for example, temperature changes, $\Delta_{CW}T$) across CCMs and for different time horizons[5,7].

In this study, we diagnosed the sensitivity of surface ozone to large-scale temperature variations (hereafter referred to as dO_3/dT_{LS}) over the SEUS as a means to understand the response of surface ozone to climate warming ($\Delta_{CW}O_3$). Figure 1a shows the August surface temperature over the SEUS (T_{SEUS}) during 1988–2011. There was no significant trend in T_{SEUS}, but oscillated interannually over a range of approximately 3 K. We found that this interannual variation (IAV) of T_{SEUS} was a manifestation of the first empirical orthogonal function (EOF) of the IAV of August surface temperature over the contiguous US during 1988–2011 (Fig. 1a, $r^2(T_{SEUS}$, first EOF) = 0.69). The first EOF of US August temperature was characterized by an oscillation where almost the entire contiguous US is in the same phase (Fig. 1c). Subsequent US August temperature EOFs were of finer spatial scales and not significantly correlated with T_{SEUS} (Fig. 1b,d). Thus, during 1988–2011 and on the interannual timescale, SEUS August surface ozone was perturbed by large-scale temperature variations, which offers a unique opportunity to diagnose dO_3/dT_{LS}. In contrast, studies have analysed the sensitivity of SEUS surface ozone to daily temperature variations[13,14], but that more likely reflects the response of ozone to synoptic weather.

Figure 2a illustrates our methodology. We examined the relationship between the interannual anomalies of August afternoon (1–5 pm) ozone (ΔO_3, relative to 1988–2011 site means) and the interannual anomalies of August mean daily maximum temperature (ΔT_{max}, relative to 1988–2011 site means) measured at 20 SEUS sites during the 5-year period between 1988 and 1992 (Fig. 2a and Supplementary Fig. 1 and Supplementary Information 1). The multi-year sampling window captured the response of ozone to the IAV of temperature. Surface ozone concentrations over the SEUS declined significantly during 1988–2011 (observed trend = −5.9 ppb per decade) as a result of US anthropogenic emission reductions. Therefore, the sampling window cannot be too long, lest the lower ozone concentrations in the later years smear the true ozone–temperature relationship. As seen in Fig. 2a, ozone and temperature anomalies were highly correlated ($r(\Delta O_3, \Delta T_{max})$ = 0.86) between 1988 and 1992. We defined the ozone–temperature sensitivity (dO_3/dT_{LS}) during this 5-year period as the slope of the best-fit line of interannual ozone anomalies versus interannual temperature anomalies ($m(\Delta O_3, \Delta T_{max}) = 4.6$ ppb K^{-1}). Previous analyses defined the ozone–temperature sensitivity as the slope of ozone versus temperature ($m(O_3, T_{max})$, Fig. 2b)[14,15]. However, for multiple sites over a large area, that definition smears the true ozone–temperature relationship ($r(O_3, T_{max}) < r(\Delta O_3, \Delta T_{max})$) owing to the spatial inhomogeneity of mean temperatures and mean ozone levels across sites (Supplementary Information 2).

Figure 3 extends the analysis in Fig. 2a and shows the ozone–temperature relationship for each of the twenty 5-year periods during 1988–2011. Observed ozone and temperature anomalies were highly correlated throughout this time (Fig. 3a, black, $r(\Delta O_3 \Delta T_{max}) = 0.60$ to 0.86, p-values < 0.01). The observed $m(\Delta O_3, \Delta T_{max})$ was consistently positive and averaged 4.6 ppb K^{-1},

[1]Laboratory for Climate and Ocean-Atmosphere Studies, Department of Atmospheric and Oceanic Sciences, School of Physics, Peking University, Beijing 100871, China. [2]Department of Geology and Geophysics, Yale University, New Haven, Connecticut 06511, USA. [3]Program in Atmospheric and Oceanic Sciences, Princeton University, Princeton, New Jersey 08544, USA. [4]Geophysical Fluid Dynamics Laboratory/National Oceanic and Atmospheric Administration, Princeton, New Jersey 08540, USA. [5]School of Engineering and Applied Sciences, Harvard University, Cambridge, Massachusetts 02138, USA. *e-mail: tmfu@pku.edu.cn

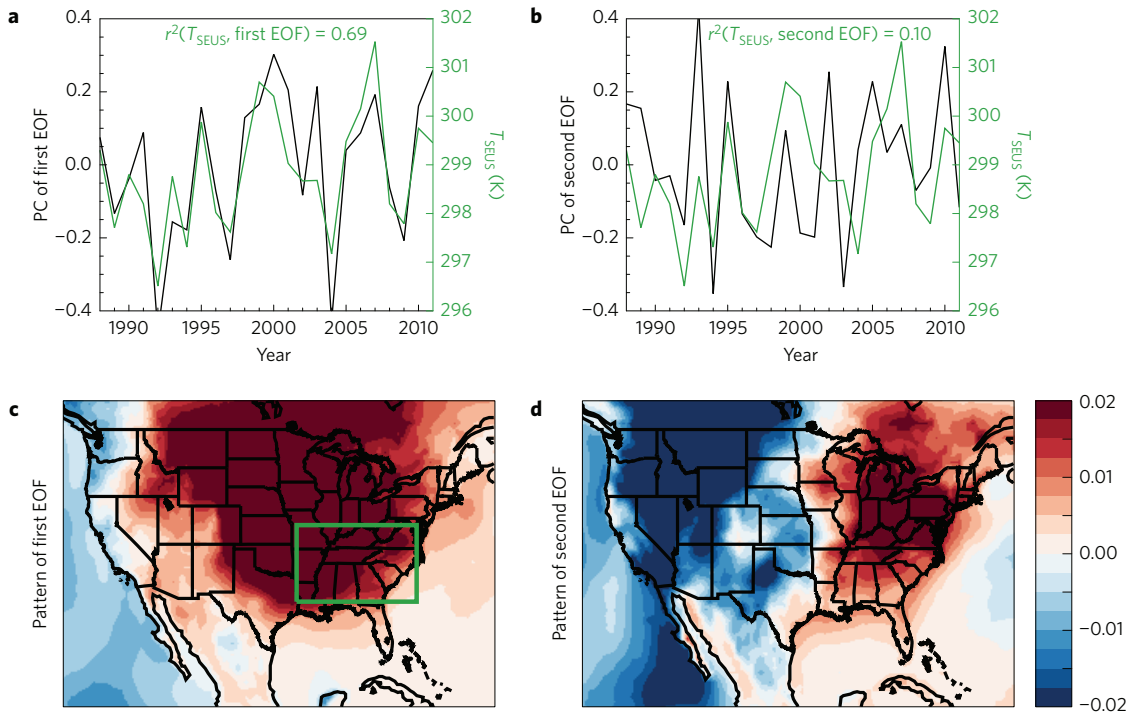

Figure 1 | SEUS temperature variations on the interannual timescale. a,**b**, The IAV of August surface temperature over the SEUS (T_{SEUS}, green) and time series of the first (**a**) and second (**b**) EOFs of US August surface temperature (black) during 1988–2011. The correlations between T_{SEUS} and the EOFs are shown inset. **c**,**d**, Spatial patterns of the first (**c**) and second (**d**) EOFs. The green box in **c** is the area where the August surface temperature was averaged to calculate T_{SEUS}.

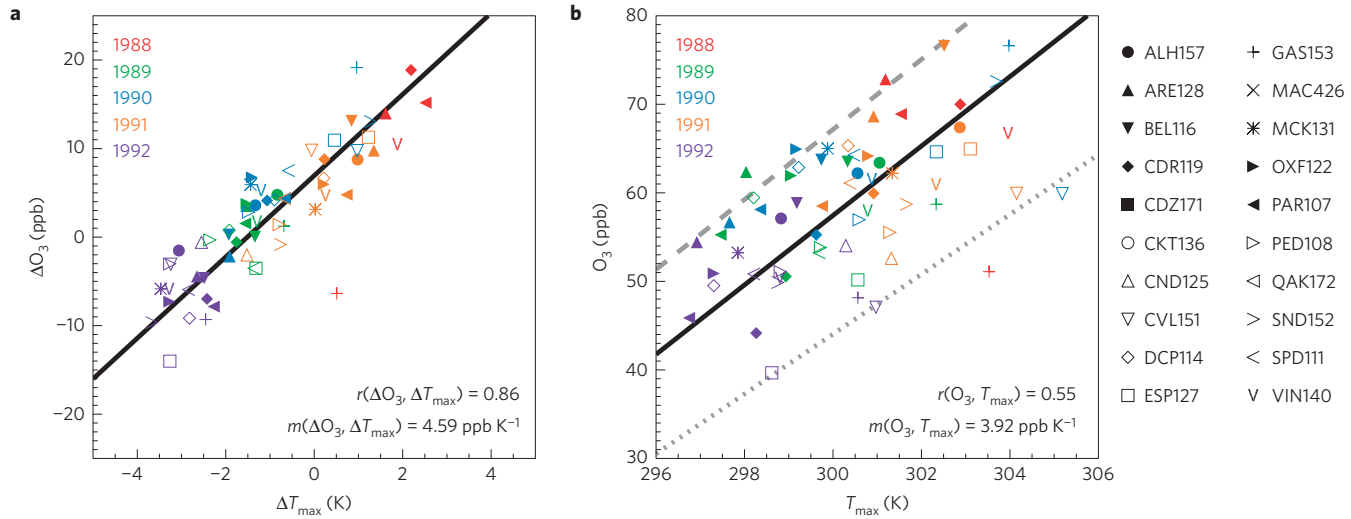

Figure 2 | Comparison of two ozone–temperature sensitivity definitions. a, In this study, sensitivity is defined as the slope ($m(\Delta O_3, \Delta T_{max})$) of the best-fit line of interannual ozone anomalies versus interannual temperature anomalies. **b**, Previous studies define sensitivity as the slope ($m(O_3, T_{max})$) of the best-fit line of ozone versus temperature, smearing the true ozone–temperature relationship. In **a** and **b** data are coded by site (symbols) and by year (colour). The black lines indicate the best-fit lines. The grey dashed and dotted lines indicate the best-fit lines for observations at ARE128 and CVL151, respectively. Correlations and slopes are shown inset.

but it varied greatly between 2.4 ppb K^{-1} and 7.1 ppb K^{-1} (Fig. 3b, black). Similar results were obtained using a longer sampling window (Supplementary Fig. 2a). Previous studies found that the ozone–temperature sensitivity (defined as $m(O_3, T_{max})$) over the Mid-Atlantic and SEUS decreased by approximately 1 ppb K^{-1} after the early 2000s and suggested US NO_x emission reductions to be the driver[14,15] (Supplementary Fig. 3). Although the results from previous studies and those from our analyses are not quantitatively comparable owing to differences in definition and sampling, we did find that $m(\Delta O_3, \Delta T_{max})$ decreased from an average of 4.9 ppb K^{-1} for the ten 5-year periods between 1988–2001 to an average of 3.3 ppb K^{-1} for the six 5-year periods between 2002–2011. However, observed $m(\Delta O_3, \Delta T_{max})$ peaked not during the earlier years (when US NO_x emissions were strongest) but during 1996–2003, suggesting that NO_x-reduction was not the sole driver for the interannual variability of $m(\Delta O_3, \Delta T_{max})$.

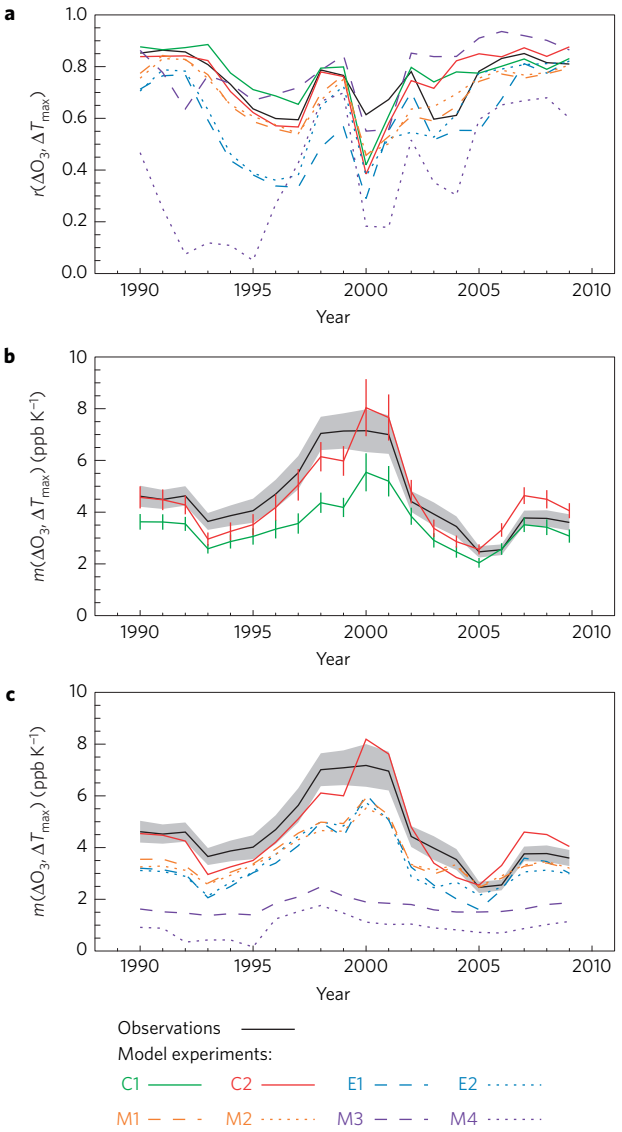

Figure 3 | Ozone–temperature relationship over the SEUS. a–c, August ozone–temperature correlations (**a**) and sensitivities (**b** and **c**) for the twenty 5-year periods during 1988–2011. Observations are shown in black; grey bands indicate standard errors. Coloured lines show model results; vertical bars indicate standard errors (Supplementary Table 1). C1 and C2: experiments assuming different isoprene photochemistry; E1: same as C2 but without the IAV of natural precursor emissions; E2: no IAV in all precursor emissions; M1: same as E2 but without the IAV of humidity in photochemistry calculations; M2: same as M1 but without the IAV of shortwave radiation and cloud cover; M3: same as M2 but without the IAV of horizontal winds; M4: same as M3 but without the IAV of temperature in photochemistry calculations.

We used a global three-dimensional chemical transport model (GEOS-Chem) to examine the drivers for the observed $m(\Delta O_3, \Delta T_{max})$ and its interannual variability. We drove the model with observation-constrained meteorological data (reanalysis). Year-specific precursor emissions were based on best knowledge at present (Supplementary Fig. 3 and Supplementary Information 3). A key uncertainty in current models is the fate of organic nitrates from isoprene oxidation (ION; refs 4,5,7,12). Oxidations of both isoprene and its carbonyl products form organic peroxy radicals (RO_2). A branch of the $RO_2 + NO$ reaction produces ION, but the yield (Y_{ION}) and the NO_x-recycling efficiency (α) upon ION oxidation are at present uncertain[16]. Together, these two parameters (Y_{ION} and α) determine the net sequestration of NO_x by ION formation[17], which in turn determines how regional ozone responds to enhanced isoprene emissions[12,18]. Moreover, the choice of Y_{ION} and α in a model should be calibrated for its model resolution, as stronger NO_x-sequestration can compensate for the enhanced ozone production efficiency associated with the diluted NO_x in a coarser model grid[12]. We conducted model experiments using two schemes for isoprene photochemistry (Supplementary Table 1 and Supplementary Information 3 and 4). In Scheme C1 (ref. 19), ION were produced as first-generation products ($Y_{ION} = 15\%$), which quickly deposited to remove NO_x ($\alpha = 0\%$). In Scheme C2, first-generation ION ($Y_{ION} = 11.7\%$) oxidized to recycle $\alpha = 55\%$ of NO_x and produced secondary organic nitrates[20]. The simulations using schemes C1 and C2 both overestimated surface ozone over the eastern US, a common problem in models[6,15]. However, for both schemes, the positive biases over the SEUS were mainly due to an overestimation of the regional ozone background by approximately 20 ppb, which although large had only minor impacts on the simulated $m(\Delta O_3, \Delta T_{max})$ (Supplementary Information 4). The C2 simulation (Fig. 3b, red) better reproduced the magnitude and variability of the observed $m(\Delta O_3, \Delta T_{max})$ at our model resolution (2.5° longitude × 2° latitude). We adopted Scheme C2 for subsequent model experiments.

We conducted model experiments removing the IAV of natural and anthropogenic emissions by using year 1988 emissions for all years (Fig. 3c). The year 1988 represents a high-NO_x-emission year with a small T_{SEUS} anomaly. We found that the IAV of natural precursor (mostly isoprene) emissions consistently acted to increase the simulated $m(\Delta O_3, \Delta T_{max})$ (Fig. 3c, differences between the red solid and blue dashed lines). Given that the $m(\Delta O_3, \Delta T_{max})$ simulated by experiment C2 were in good agreement with the observed $m(\Delta O_3, \Delta T_{max})$, our analysis gives evidence for isoprene having a positive contribution to dO_3/dT_{LS}, which has been a major uncertainty in previous CCM studies[4,5,7]. In contrast to previous postulations[14,15], we found that the US anthropogenic emission reductions after the early 2000s had only small impacts on the simulated $m(\Delta O_3, \Delta T_{max})$ (Fig. 3c, differences between the blue dashed and blue dotted lines), insufficient to explain the large interannual variability of the observed $m(\Delta O_3, \Delta T_{max})$. These findings remain valid when a longer sampling window was used (Supplementary Fig. 2a), in experiments where the emissions were locked to a low-NO_x-emission year (Supplementary Fig. 2b), and in experiments where the order of the natural and anthropogenic emission IAV removal was reversed (Supplementary Fig. 2c).

Even without the IAV of precursor emissions, there remained a large interannual variability in the simulated $m(\Delta O_3, \Delta T_{max})$ (Fig. 3c, blue dotted line), most likely driven by the IAV of meteorology. We conducted experiments decoupling the IAV of meteorological variables (by using year 1988 meteorological data for all years). Previous studies found a negative correlation between humidity and ozone over the SEUS (refs 13,21). We wondered whether this was due to the impacts of humidity on ozone photochemistry[4] and whether it would be a key driver in the interannual variability of $m(\Delta O_3, \Delta T_{max})$. However, removing the IAV of humidity in photochemistry calculations led to only small changes in the simulated ozone and $m(\Delta O_3, \Delta T_{max})$ (Fig. 3c, differences between the blue dotted and orange dashed lines). The impacts of the IAV of cloud and shortwave radiation on simulated $m(\Delta O_3, \Delta T_{max})$ were also limited (Fig. 3c, differences between the two orange lines). We found, however, that the increased advection of ozone into the SEUS coupled to large-scale warming was an important driver for both the magnitude and the variability of $m(\Delta O_3, \Delta T_{max})$ (diagnosed by the difference between simulations using annually varying horizontal winds versus year 1988 horizontal winds; the differences between the orange dotted and purple

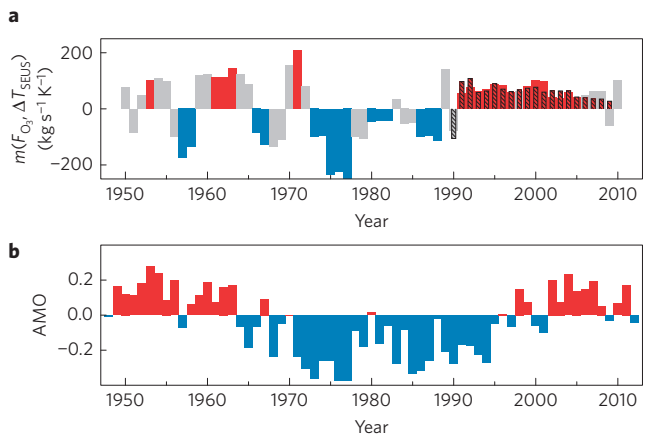

Figure 4 | IAV of the coupling between regional ozone advection and temperature. a, Sensitivity ($m(F_{O_3}, \Delta T_{SEUS})$) of the net ozone mass flux advected into the SEUS boundary layer (F_{O_3}) to the interannual anomaly of SEUS surface temperature (ΔT_{SEUS}, detrended). Solid bars: F_{O_3} calculated from simulated 1988 ozone concentrations (C2) and observed 1948–2012 winds. Hatched bars: F_{O_3} calculated from year-specific simulations (C2). Red and blue bars indicate significant positive and negative sensitivities, respectively (p-value < 0.1). Grey bars indicate nonsignificant sensitivities. **b**, Atlantic Multidecadal Oscillation (AMO) index. Red and blue bars indicate positive and negative anomalies, respectively.

dashed lines in Fig. 3c). Finally, the impacts of temperature on photochemical reaction rates contributed approximately 1 ppb K^{-1} to the overall ozone–temperature sensitivity (Fig. 3c, differences between the two purple lines). These results hold true when a longer sampling window was used and when the meteorology was locked to a different year (Supplementary Fig. 2a,b).

Our results showed that, even without the IAV in precursor emissions, variation in ozone advection by regional circulation can lead to large interannual variability in the sensitivity of ozone to large-scale warming (dO_3/dT_{LS}). To examine this over a longer period, we extrapolated the net August ozone mass fluxes advected into the SEUS boundary layer (F_{O_3}) during 1948–2012 using simulated ozone concentrations for August 1988 and reanalysis winds during August 1948–2012. We then calculated the sensitivity ($m(F_{O_3}, \Delta T_{SEUS})$) of these ozone fluxes (F_{O_3}) to the interannual anomalies of August surface temperature over the SEUS (ΔT_{SEUS}, detrended) during each 5-year period between 1948–2012 (Fig. 4a, solid bars). $m(F_{O_3}, \Delta T_{SEUS})$ was mostly positive during 1988–2011. This is consistent with our model experiments, which showed that regional ozone advection enhanced the ozone–temperature sensitivity over the SEUS during 1988–2011 (Fig. 3c). However, $m(F_{O_3}, \Delta T_{SEUS})$ varied greatly over the past 60 years and changed signs on interannual to interdecadal timescales. Negative $m(F_{O_3}, \Delta T_{SEUS})$ (for example, during 1973–1988) may partially offset the impacts of isoprene on ozone, reducing the overall ozone–temperature sensitivity. The variability of US summer meteorology is correlated with the Atlantic Multidecadal Oscillation (AMO; refs 22,23) and other climate indices[24]. We found the correlation between $m(F_{O_3}, \Delta T_{SEUS})$ and the AMO (Fig. 4b) to be 0.41. Although not extremely high, this correlation is significant (p-value $= 0.08$, taking into account the serial correlations inherent in both time series[25]), indicating a possible link between air quality and interdecadal climate variability. A general circulation model study examined the atmospheric responses to ocean temperature forcings associated with the AMO (ref. 26). That study found that positive and negative AMO phases lead to enhancements of northeasterly and southwesterly surface winds over the SEUS, respectively. This may result in advection of high-ozone air into the SEUS from the Northeast US during positive AMO and low-ozone air from the Gulf of Mexico during negative AMO, potentially explaining our result. This possible linkage between SEUS surface ozone and the AMO is still uncertain and warrants further study.

The positive, but variable, sensitivity of ozone to large-scale warming (dO_3/dT_{LS}) reported here is a relevant diagnosis of the response of ozone to climate warming for polluted forested areas, especially for the near-term. Additional ecosystem processes not addressed here, such as CO_2-inhibition of biogenic emissions and land-cover changes due to climate warming, may become increasingly important further into the future[27,28]. Our results help explain the lack of consensus among previous CCM predictions of $\Delta_{CW}O_3$. In addition to uncertainties in precursor photochemistry and predicted regional climate changes (for example, $\Delta_{CW}T$), dO_3/dT_{LS} is interannually and interdecadally variable, such that $\Delta_{CW}O_3 \sim (dO_3/dT_{LS}) \cdot \Delta_{CW}T$ could be wide-ranging across CCMs and for different time horizons. Prediction of future ozone changes will require CCMs with more realistic representations of climate variability and its drivers, such as models initialized with observed ocean conditions[29]. Long-term management of ozone air quality must consider the variability of dO_3/dT_{LS} to ensure consistent attainment of ozone air quality standards in the future.

Methods

MERRA data set. The Modern Era Retrospective-analysis for Research and Applications (MERRA) assimilated meteorological data set is from the NASA Global Modeling and Assimilation Office (http://gmao.gsfc.nasa.gov/research/merra). The native resolution of MERRA is 0.667° longitude × 0.5° latitude with 72 vertical layers. The temporal resolution of MERRA is 3 h for atmospheric variables and 1 h for surface variables.

Observations. Co-located, hourly surface ozone and temperature measurements are from the Clean Air Status and Trends Network (CASTNET; ref. 30) managed by the US Environmental Protection Agency (http://www.epa.gov/castnet). We selected 20 sites (Supplementary Fig. 1) in the SEUS (90°–76° W, 31°–40° N) that are rural, non-mountainous, not affected by local land–sea breeze, and with at least 18 years' worth of valid August mean afternoon (1–5 pm local time) surface ozone and August mean daily maximum temperature measurements during 1988–2011. Interannual anomalies of August mean afternoon ozone concentration (ΔO_3) and August mean daily maximum temperature (ΔT_{max}) at each site were calculated by removing the long-term (1988–2011) means at that site.

Model description. We used the GEOS-Chem model (v9-01-02, http://geos-chem.org) to simulate global ozone concentrations during 1988–2011. GEOS-Chem is driven by a regridded MERRA data set where the horizontal resolution of the MERRA data was downgraded to 2.5° × 2° and the number of vertical levels of the MERRA data was reduced to 47 levels. We drove the model with year-specific ozone precursor emissions based on best knowledge at present (Supplementary Fig. 3 and Supplementary Information 3). In particular, biogenic volatile organic compounds (VOC) emissions were calculated by the Model of Emissions of Gases and Aerosols from Nature (MEGAN) and dependent on temperature, shortwave radiation and monthly leaf area index[11]. The standard HO_x–NO_x–VOC–ozone–aerosol chemical mechanism (except the isoprene photochemical cascade) used in GEOS-Chem is as described by ref. 19 with a number of recent updates. We conducted model experiments using two different schemes for the isoprene photochemical cascade. Scheme C1 is as described in ref. 19. Scheme C2 is based on a recent experimental study[20]. We conducted additional model experiments by progressively removing the IAV of various emission sources and meteorological variables (Supplementary Table 1). We removed the IAV of precursor emissions from a specific source by using fluxes from that source from the year 1998 for all years. Natural emissions were locked to 1998 levels by driving the MEGAN algorithm and the soil NO_x emission algorithm with temperature, sunlight and precipitation data from the year 1988. We removed the IAV of a specific meteorological field by using values for that meteorological field from the year 1988 for all years. All model experiments were conducted from January 1988 to August 2011. Results for the month of August were analysed.

Ozone–temperature sensitivity. The sensitivity of ozone to temperature ($m(\Delta O_3, \Delta T_{max})$) was defined as the slope of the reduced major-axis regression line for ozone anomaly (ΔO_3) versus temperature anomaly (ΔT_{max}) sampled from the neighbouring five years. Correlations, slopes, and standard errors were

calculated using the bootstrap technique (resampling 500 times with replacements). Simulated sensitivities were calculated by sampling the model outputs at the locations of CASTNET sites where valid observations were available for that month.

1948–2012 ozone mass flux. We calculated the net ozone mass flux into the SEUS (93.75° W–76.25° W, 31° N–39° N) boundary layer (surface to 850 hPa) during August 1948–2012 using simulated 1988 ozone concentrations (experiment C2) and assimilated winds from the National Center for Environmental Prediction (NCEP) Reanalysis 1 data set from the National Oceanic and Atmospheric Administration/Earth System Research Laboratory (NOAA/ESRL) (http://www.esrl.noaa.gov/psd). The sensitivity of net ozone mass flux to temperature was defined as the slope of the best-fit line ($m(F_{O_3}, \Delta T_{SEUS})$) of net ozone mass flux (F_{O_3}) to the interannual anomaly of August surface temperature over the SEUS (ΔT_{SEUS}, detrended) sampled from the neighbouring 5-year period.

AMO index. Unsmoothed and detrended monthly AMO indices for 1948–2012 were from the NOAA/ESRL (http://www.esrl.noaa.gov/psd/data/timeseries/AMO).

Received 3 May 2014; accepted 9 February 2015; published online 23 March 2015

References

1. Jerrett, M. *et al.* Long-term ozone exposure and mortality. *N. Engl. J. Med.* **360,** 1085–1095 (2009).
2. Fowler, D. *et al.* Atmospheric composition change: Ecosystems–atmosphere interactions. *Atmos. Environ.* **43,** 5193–5267 (2009).
3. Racherla, P. N. & Adams, P. J. Sensitivity of global tropospheric ozone and fine particulate matter concentrations to climate change. *J. Geophys. Res.* **111,** D24103 (2006).
4. Jacob, D. J. & Winner, D. A. Effect of climate change on air quality. *Atmos. Environ.* **43,** 51–63 (2009).
5. Fiore, A. M. *et al.* Global air quality and climate. *Chem. Soc. Rev.* **41,** 6663–6683 (2012).
6. Doherty, R. M. *et al.* Impacts of climate change on surface ozone and intercontinental ozone pollution: A multi-model study. *J. Geophys. Res.* **118,** 3744–3763 (2013).
7. Weaver, C. P. *et al.* A preliminary synthesis of modeled climate change impacts on US regional ozone concentrations. *Bull. Am. Meteorol. Soc.* **90,** 1843–1863 (2009).
8. Wu, S., Mickley, L. J., Jacob, D. J., Rind, D. & Streets, D. G. Effects of 2000–2050 changes in climate and emissions on global tropospheric ozone and the policy-relevant background surface ozone in the United States. *J. Geophys. Res.* **113,** D18312 (2008).
9. Langner, J. *et al.* A multi-model study of impacts of climate change on surface ozone in Europe. *Atmos. Chem. Phys.* **12,** 10423–10440 (2012).
10. Wu, S. *et al.* Effects of 2000–2050 global change on ozone air quality in the United States. *J. Geophys. Res.* **113,** D06302 (2008).
11. Guenther, A. *et al.* Estimates of global terrestrial isoprene emissions using MEGAN (Model of Emissions of Gases and Aerosols from Nature). *Atmos. Chem. Phys.* **6,** 3181–3210 (2006).
12. Ito, A., Sillman, S. & Penner, J. E. Global chemical transport model study of ozone response to changes in chemical kinetics and biogenic volatile organic compounds emissions due to increasing temperatures: Sensitivities to isoprene nitrate chemistry and grid resolution. *J. Geophys. Res.* **114,** D09301 (2009).
13. Camalier, L., Cox, W. & Dolwick, P. The effects of meteorology on ozone in urban areas and their use in assessing ozone trends. *Atmos. Environ.* **41,** 7127–7137 (2007).
14. Bloomer, B. J., Stehr, J. W., Piety, C. A., Salawitch, R. J. & Dickerson, R. R. Observed relationships of ozone air pollution with temperature and emissions. *Geophys. Res. Lett.* **36,** L09803 (2009).
15. Rasmussen, D. J. *et al.* Surface ozone-temperature relationships in the eastern US: A monthly climatology for evaluating chemistry-climate models. *Atmos. Environ.* **47,** 142–153 (2012).
16. Perring, A. *et al.* Airborne observations of total $RONO_2$: New constraints on the yield and lifetime of isoprene nitrates. *Atmos. Chem. Phys.* **9,** 1451–1463 (2009).
17. Paulot, F., Henze, D. & Wennberg, P. Impact of the isoprene photochemical cascade on tropical ozone. *Atmos. Chem. Phys.* **12,** 1307–1325 (2012).
18. Fiore, A. M., Levy, H. II & Jaffe, D. A. North American isoprene influence on intercontinental ozone pollution. *Atmos. Chem. Phys.* **11,** 1697–1710 (2011).
19. Horowitz, L. W., Liang, J., Gardner, G. M. & Jacob, D. J. Export of reactive nitrogen from North America during summertime: Sensitivity to hydrocarbon chemistry. *J. Geophys. Res.* **103,** 13451–13476 (1998).
20. Paulot, F. *et al.* Isoprene photooxidation: New insights into the production of acids and organic nitrates. *Atmos. Chem. Phys.* **9,** 1479–1501 (2009).
21. Blanchard, C., Hidy, G. & Tanenbaum, S. NMOC, ozone, and organic aerosol in the southeastern United States, 1999–2007; 2. Ozone trends and sensitivity to NMOC emissions in Atlanta, Georgia. *Atmos. Environ.* **44,** 4840–4849 (2010).
22. Rogers, J. C. The 20th century cooling trend over the southeastern United States. *Clim. Dynam.* **40,** 341–352 (2013).
23. Sutton, R. T. & Hodson, D. L. Atlantic Ocean forcing of North American and European summer climate. *Science* **309,** 115–118 (2005).
24. Li, W. H., Li, L. F., Fu, R., Deng, Y. & Wang, H. Changes to the North Atlantic Subtropical High and its role in the intensification of summer rainfall variability in the Southeastern United States. *J. Clim.* **24,** 1499–1506 (2011).
25. Ebisuzaki, W. A method to estimate the statistical significance of a correlation when the data are serially correlated. *J. Clim.* **10,** 2147–2153 (1997).
26. Sutton, R. T. & Hodson, D. L. R. Climate response to basin-scale warming and cooling of the North Atlantic Ocean. *J. Clim.* **20,** 891–907 (2007).
27. Sanderson, M., Jones, C., Collins, W., Johnson, C. & Derwent, R. Effect of climate change on isoprene emissions and surface ozone levels. *Geophys. Res. Lett.* **30,** 1936 (2003).
28. Rosenstiel, T. N., Potosnak, M. J., Griffin, K. L., Fall, R. & Monson, R. K. Increased CO_2 uncouples growth from isoprene emission in an agriforest ecosystem. *Nature* **421,** 256–259 (2003).
29. Taylor, K. E., Stouffer, R. J. & Meehl, G. A. An overview of CMIP5 and the experiment design. *Bull. Am. Meteorol. Soc.* **93,** 485–498 (2012).
30. Clark, T. L. & Karl, T. R. Application of prognostic meteorological variables to forecasts of daily maximum one-hour ozone concentrations in the northeastern United States. *J. Appl. Meteorol.* **21,** 1662–1671 (1982).

Acknowledgements

T-M.F. was supported by the Ministry of Science and Technology of China (2014CB441303) and the National Natural Science Foundation of China (41222035, 41175101). F.P. was supported by the Harvard University Center for the Environment. J.M. was supported in part by the NOAA Climate Program Office (NA13OAR4310071). GEOS-Chem is managed by the Harvard University Atmospheric Chemistry Modeling Group with support from the NASA Atmospheric Composition Modeling and Analysis Program. We thank M. Cooper and R. Martin of Dalhousie University for providing the 2.5° × 2° resolution MERRA data.

Author contributions

T-M.F. designed the study, performed the simulations and analyses, and wrote the paper. Y.Z. assisted in the data analysis. F.P. and J.M. developed and implemented the new isoprene photochemistry scheme for GEOS-Chem. R.M.Y. developed the capability of driving GEOS-Chem with the MERRA data. All authors discussed the paper.

Additional information

Supplementary information is available in the online version of the paper. Reprints and permissions information is available online at www.nature.com/reprints. Correspondence and requests for materials should be addressed to T-M.F.

Competing financial interests

The authors declare no competing financial interests.